Nonlinear Light Microscopy by a 1.2-μm Fiber-Laser-Based Femtosecond Dispersive Wave Source

Hsien-Yi Wang
Shiuan-Wen Huang
Dean-Ru Li
Bor-Shyh Lin
Ming-Che Chan
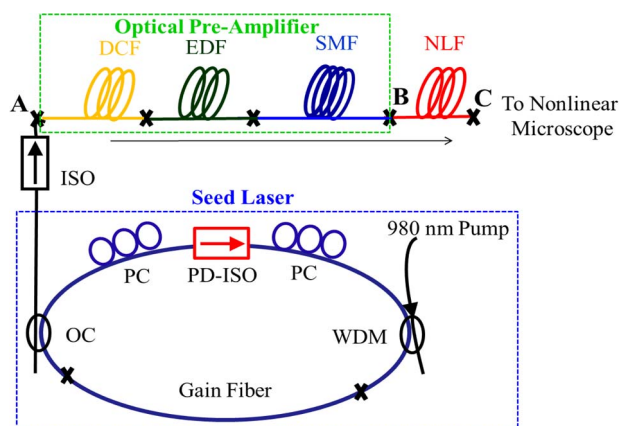
Nonlinear Light Microscopy by a 1.2-μm Fiber-Laser-Based Femtosecond Dispersive Wave Source

Hsien-Yi Wang,[1,2] **Shiuan-Wen Huang,**[3] **Dean-Ru Li,**[3]
Bor-Shyh Lin,[3] **and Ming-Che Chan**[3]

[1]Department of Nephrology, Chi-Mei Medical Center, Tainan 710, Taiwan
[2]Department of Sports Management, College of Leisure and Recreation Management,
Chia Nan University of Pharmacy and Science, Tainan 717, Taiwan
[3]College of Photonics, National Chiao-Tung University, Tainan 71150, Taiwan

Abstract: A fiber-laser-based femtosecond dispersive wave laser source, operated within the 1.2- to 1.3-μm bio-penetration wavelength window, and its application on nonlinear light microscopy were both demonstrated in this paper. This portable 1.2-μm femtosecond fiber-optic source was composed of an all-fiber 1.55-μm mode-locked erbium-doped fiber laser as the excitation source and a nonlinear fiber as a frequency up converter. The 1.2-μm femtosecond radiations with an up to a 55-mW output power and a 125-fs pulsewidth were experimentally demonstrated. By the fiber-based 1.2-μm femtosecond dispersive wave source, nonlinear laser scanning microscopy, including two-photon fluorescence and second-harmonic generation microscopy, was also performed within the 1.2- to 1.3-μm bio-penetration window in this report. The fiber-based 1.2-μm femtosecond light source, with a simple system configuration, turn-key operation, and a miniaturized package, shows great potential for nonlinear light microscopy and other related applications outside of the laboratory.

Index Terms: Fiber laser, dispersive wave, passive mode-locking, nonlinear microscopy, nonlinear fiber optics, bio-photonics.

1. Introduction

Advanced by near-infrared femtosecond lasers, nonlinear light microscopy (NLM) has demonstrated great medical and biological capability to provide molecular and structural information with high 3-D spatial resolution [1]. By different nonlinear interactions mechanisms of femtosecond laser pulses with at least sub-nJ pulse energies inside specimens, various NLM techniques and corresponding applications, including higher harmonic fluorescence microscopy [1]–[4], higher harmonic generation microscopy [5]–[8], coherent-anti-Stoke Raman scattering (CARS) microscopy [9], and stimulated-Raman scattering (SRS) microscopy [10], have been demonstrated by many different groups.

In NLM, selecting proper excitation wavelength is always the key issue because the excitation wavelength was related with imaging penetration depth and sample viability [2]–[6]. The imaging

penetration depth in NLM is determined by absorption and scattering effects of photons within the biological tissues. Light absorption within biological tissues is dominated by the absorption of water while light scattering becomes weaker as increasing the excitation wavelength. To maximize penetration depth, the wavelength selection of the excitation laser should be the best trade-off between absorption and scattering [11]. From previous studies in most biological tissues, the optimal laser penetration window, called the bio-penetration window, is located at the 1.2–1.3 μm wavelength regimes [3], [6], [11], [12]. Recently, enabled by 1200–1300 nm femtosecond light sources, including Cr:forsterite lasers [5], [6] and optical parametric oscillators (OPO) [3], sectioned nonlinear microscopy images were demonstrated to provide the molecular and structural information with a > 1 mm penetration depth and 3-D sub-micron resolutions. Within the 1200–1300 wavelength windows, the much reduced photo damage also increases the sample viability [2], [6]. Moreover, the near 1300 nm excitation wavelength corresponds to zero dispersion wavelengths in Silica fibers, making fiber-based NLM system possible [5], [12].

Besides proper excitation wavelength, for future biomedical and even clinical applications outside of the laboratory, a compact, portable, low cost and easily-operated 1200–1300 nm femtosecond light sources is highly desirable [12]. However, current solid-state light sources working in the 1.2–1.3 μm bio-penetration window, including mode-locked Cr:forsterite lasers and OPOs, are usually with bulky layouts, complicated pumping, cooling, and maintained setups. During successive operations, the precise and careful opto-mechanical adjusting and maintaining procedures are usually necessary. Moreover, water-cooled systems, instead of air-cooled systems, are needed to remove the heat from the gain crystals in Cr:forsterite lasers and OPOs. The issues addressed above limits the future possible bio-medical or even clinical applications outside of the laboratory.

Previous studies on fiber-based systems and mode-locked lasers show that femtosecond fiber-based light sources offer several advantages over traditional bulk solid-state lasers, including higher electrical-optical conversion efficiencies, lower cost, more compact system arrangement, more flexible light delivery, greater stability due to better isolation from environmental perturbations such as noises and dusts, and more-efficient heat-removal mechanisms allowing the scaling of laser power and brightness [13]. Furthermore, according to the waveguide nature of fiber lasers, the output mode pattern from fiber lasers is close to an ideal point source and the alignment sensitivity is greatly reduced for maintenance-free operations in clinical applications. Although femtosecond fiber lasers have been well developed in the 1.0 μm wavelength regime by mode-locked Ytterbium fiber lasers [14], in the 1.55 μm wavelength regime by mode-locked Erbium fiber lasers [15] and in the 1.9–2.0 μm wavelength regime by mode-locked Thulium fiber lasers [16], to our best of knowledge, there are few femtosecond fiber lasers directly worked within the 1.2 $\sim$ 1.3 μm bio-penetration window, which is very suitable for NLM.

On the other hand, optical fibers can also be as an efficient wavelength convertor by dispersive wave (DW) generation. This nonlinear fiber optical effect originates from the interactions of higher-order fiber dispersion and solitons propagating in the anomalous fiber dispersion regime (D > 0). Recently, based on various nonlinear fibers, several groups have demonstrated DW-based femtosecond light source by different excitation wavelength and nonlinear fiber. Kartner's group have demonstrated highly efficient 0.4 μm DW based on a 10 fs Ti:Sapphire laser [17]. On the other hand, based on mode-locked Ytterbium fiber lasers as an excitation source, some groups have reported fiber-based DW sources. Liu *et al.* has reported a 0.58–0.63 μm DW [18] with a 4.8 mW maximum DW power while Nishizawa's group has demonstrated a 0.6–0.68 μm DW with a $\sim$1 mW DW power [19]. In 2015, a highly efficient tunable 1.63 $\sim$ 1.68 μm DW have been reported where an optical parametric oscillator (OPO) working at 1.76 μm was used as excitation and a Tellurite microstructured fiber was utilized as a wavelength up convertor [20]. Compared with other's work, the reported optical power was high-enough to perform NLM. However, an OPO is not compact and easily tunable. Moreover, to our best knowledge, there are no suitable fiber-based DW sources working within the 1.2 $\sim$ 1.3 μm wavelength regime for NLM applications.
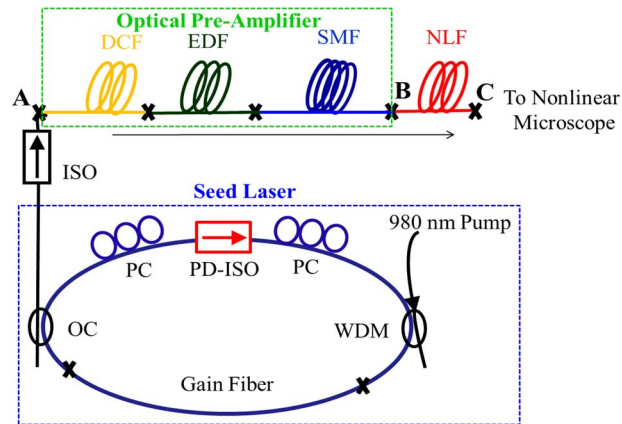
Fig. 1. Schematic representation of the fiber-based femtosecond 1.2 μm dispersive wave source. The seed fiber laser is enclosed in the blue-dashed box, and the optical pre-amplifier is enclosed in the green-dashed box. The seed fiber laser (enclosed in the blue-dashed box) was utilized to generate 1.55 μm femtosecond pulses. The home-made optical pre-amplifier (enclosed in the green-dashed box) was utilized to raise the pulse energy of 1.55 μm femtosecond pulses. The nonlinear fiber (shown in the red-colored line) was used for wavelength conversion from the 1.55 μm to 1.2 μm range through the DW generation process. The generated 1.2 μm DW pulses were then connected to the nonlinear microscope (FV-300, Olympus) to perform two-photon fluorescence and second-harmonic-generation microscopy. The auto-correlation traces and spectrum were measured at point A, B, and C for sequentially characterizing the output performances of the seed laser, pre-amplifier, and nonlinear fiber. OC: output coupler; PC: polarization controller; WDM: wavelength-division multiplexer; ISO: isolator; PD-ISO: polarization-dependent isolator; DCF: dispersion-compensation fiber; EDF: Erbium-doped fiber; SMF: single-mode fiber; NLF: nonlinear fiber.

In this paper, based on an Erbium-doped all-fiber femtosecond laser as the excitation source and a nonlinear fiber as the wavelength convertor through DW generation process, we present a fiber-based femtosecond DW source within the 1.2~1.3 μm bio-penetration window. The average power of the femtosecond DW source was multi-tens of milliwatt-level and a pulse-duration of 125 fs. With the demonstrated light source, two-photon fluorescence microscopy (TPF) and second-harmonic generation (SHG) microscopy on bio-tissues were performed. These demonstrated experimental results show that the fiber-based femtosecond DW source, working within the 1.2~1.3 μm bio-penetration window, shows great promises to serve as excitation sources for nonlinear light microscopy because the fiber-optic source is simple in configuration, with low operation/maintenance difficulty and a lower cost, and provides a flexible and reliable light delivery to the nonlinear microscope.

2. Experimental Details

The layout of the compact fiber-based femtosecond 1.2 μm DW source is shown in Fig. 1. The laser was composed of a femtosecond seed fiber laser (enclosed in the blue-dashed box), a home-made optical pre-amplifier (enclosed in the green-dashed box), and a nonlinear fiber. The seed laser and the home-made optical pre-amplifier were used for generating excitation medium power 1.55 μm femtosecond pulses. In addition, the nonlinear fiber, which is shown in the red-colored line, was used for wavelength conversion from 1.55 μm to 1.2 μm range through the DW generation process. The generated 1.2 μm DW pulses were then connected to the nonlinear microscope (FV-300, Olympus) to perform TPF and SHG microscopy.

The seed fiber laser, as shown in the blue dashed box of Fig. 1, was composed of a 980 nm pump source with a 160 mW output power, a 980/1550 wavelength division multiplexer (WDM), a 75.5-cm-long Erbium-doped fiber (EDF-80, OFS), a 20/80 output coupler (OC), two all-fiber polarization controllers (PCs), and a polarization-dependent isolator (PD-ISO). All components in the seed laser cavity are fiber-based for stable and maintaining-free laser operation. The total cavity length of the seed laser was 381.2 cm, including a 75.5-cm-long Erbium-doped fiber

providing a normal dispersion and a 305.7-cm-long single-mode fiber (SMF-28, Corning) providing an anomalous dispersion. The calculated net dispersion of seed fiber laser was -0.0106 ps^2 and the measured fundamental repetition rate was 52.4 MHz. In the seed laser, the mode-locking mechanism for generating ultrafast pulses was polarization-rotation additive pulse mode-locking (P-APM) [21], [22]. The fibers in the laser cavity and PD-ISO form a non-linear interferometer to achieve pulse-shorting. Two PCs were utilized to control the intensity bias in the nonlinear interferometer. The uni-directional ring configuration, established by the PD-ISO, was adopt for laser self-starting [21]. The net laser cavity dispersion was close to zero, which was achieved by the balance of a huge normal dispersion from Erbium-doped fiber and a huge anomalous dispersion from the rest cavity (mainly the single-mode fiber (SMF-28, Corning) fiber. The dispersion map of the seed laser cavity is helpful for stretched pulsed mode-locking which greatly reduces the round-trip nonlinear phase shift of the laser pulses and thus increase the corresponding mode-locking pulse energy [22]. The seed fiber laser was put within a clear acrylic case to prevent the possible environmental air turbulence which will destroy the mode-locking by introducing extra fiber-birefringence. In this experiment, during the whole imaging process, the laser was seem to be stable because the image quality remains stable. In the worst case, during repetitive start-up of the laser between days or when the mode-locking was quenched, the re-mode-locking process of can be quickly finished within 3–5 minutes by simply rotating the two PCs. Thus, for ultrafast pulse generation, this home-built seed laser was self-started, maintenance-free and routinely stable over several days.

Then the output from the seed laser was connected to a home-made optical pre-amplifier through an isolator (ISO). By the ISO, backward reflections after the seed laser were blocked to avoid destroying the mode-locking in the seed laser. As shown in the green dashed box of Fig. 1, the optical pre-amplifier was consisted of a 1 meter dispersion compensation fiber (DCF), a 1.4 meter Erbium-doped fiber (EDF) with a 110 dB per meter absorption (Er110-4/125, Thorlabs), and a 212 cm single mode fiber (SMF). To raise the output power of the optical pre-amplifier, the output pulses from the ISO was pre-chirped by the DCF to perform chirped-pulse amplification in the EDF [23], [24]. The EDF was forward pumped by a high power 980 nm laser diode and backward pumped by a 1480 nm laser diode. In the bi-directionally pumped scheme, the maximum output power of the forward (backward) pumping laser was 750 mW (320 mW). After the EDF, a piece of single mode fiber (SMF) with anomalous dispersion was used for pulse compression. To prevent reflections back into the amplifier, the output lead of SMF was angle cleaved. The output spectrum and pulse width from the pre-optical amplifier were measured, as shown in the point B.

The amplified output pulses from the optical pre-amplifier were than coupled into a highly non-linear fiber (shown in red lines) by two miniaturized aspheric lens. The highly nonlinear fiber (HNLF standard, OFS) is with a $\sim$3.9 μm mode-field diameter, a 11.5 W$^{-1} \bullet$ km^{-1} nonlinear coefficient and a $\sim$0.019 $\pm$ 0.004 ps/(nm$^2 \bullet$ km) dispersion slope efficiency at 1550 nm [25]. The dispersion plot of the NLF from 1.4 μm to 1.8 μm wavelength regime was also reported in [26]. The fiber was functioned as the nonlinear wavelength up-convertor from 1550 nm regime to the 1.2–1.3 μm bio-penetration window through the nonlinear process of dispersive wave generation. The fiber-delivered 1.2 μm femtosecond DW pulses were directly connected to the input of the multi-modality nonlinear microscope. Including the driving electronics, the entire 1.2 μm fiber-based femtosecond laser can be packaged within a 50 cm by 50 cm by 60 cm box.

3. Performances of the Fiber-Based Femtosecond Source

To characteristic the performance of the seed laser, several measurement was measured at point A of Fig. 1. Fig. 2(a) and (b) shows the output spectrum and auto-correlation traces of the seed laser. From the measurement, the output pulses from the seed laser were with a 293 fs pulse width and with $\sim$13 nm full-width-half-maximum (FWHM) bandwidth centered at 1554.9 nm. The average output power from the seed laser was 3.7 mW, and no signs of double-pulsing and Q-switch mode-locking were observed. According to the 52.4 MHz basic repetition rate of the seed laser, the output energy of the seed laser was 0.071 nJ.
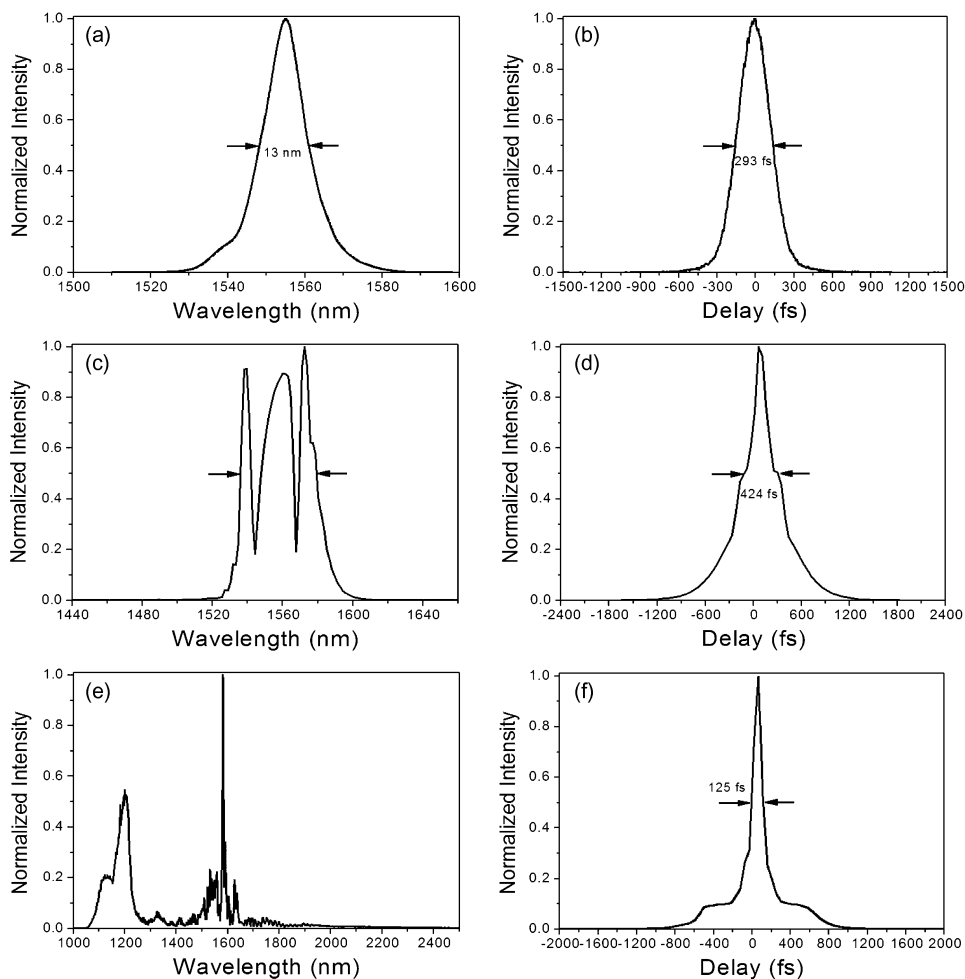
Fig. 2. (a) Spectral and (b) autocorrelation measurements from the output of seed laser. (c) Spectral and (d) autocorrelation measurements from the output of pre-optical amplifier. (e) Spectral and (f) autocorrelation measurements from the output of the nonlinear fiber.

To performing nonlinear light microscopy, the pulse energy of the excitation laser should be on the order of nJ. Thus, optical amplification of seed laser pulses is necessary. In this experiment, the seed laser pulses were launched into a 1.4 meter Erbium-doped fiber (EDF) with an extremely-high pump absorption constant (110 dB/meter). In this design, to reduce the dispersion and nonlinear effect between the amplified seed pulses and EDF, the length of EDF was reduced by selecting a high-gain fiber. Due to its high pump absorption coefficient, the EDF was forward and backward pumped by a high power 980 nm laser diode and a high power 1480 nm laser diode, respectively. Before the EDF, for chirp-pulse amplification, the amount of pre-chirp was controlled by a 1-meter dispersion compensation fiber (DCF). Then, the single-mode EDF provides the gain, as well as the spectral broadening from the fiber nonlinearities, and pulse-broadening from the normal dispersion. After the EDF, a piece of single mode fiber (SMF) with anomalous dispersion was utilized for temporal pulse compression. By carefully tuning the length of SMF after the EDF by measuring the output spectrum and the auto-correlation, for de-chirping amplified pulses, the final length of SMF inside the optical pre-amplifier was 212-cm-long. Fig. 2(c) and (d) shows the output spectrum and auto-correlation traces of the optical pre-amplifier. From the measurement, the amplified pulses were with a 424 fs pulse width and with ~44 nm FWHM bandwidth from 1535 to 1579 nm. The average output power from the seed laser was 170 mW, corresponding to a 3.24 nJ pulse energy and a 7.64 kW

peak power. The output pulses from the pre-amplifier are not non-transform-limited, which is due to the linear and nonlinear chirp induced by the fiber-nonlinearities during the pulse amplification and compression stage [27]. In Addition, the nonlinear-chirp cannot be completely compressed by a single fiber.

For generating the femtosecond fiber-delivered DW sources within the $1.2 \sim 1.3$ μm bio-penetration window, the optimum compressed 1550 nm femtosecond pulses were coupled into a 20-cm-long nonlinear fiber (HNLF standard, OFS) with a $\sim$3.9 μm mode-field diameter by two miniaturized aspheric lens pair. For the applications of nonlinear light The maximum output power was 103 mW, corresponding to a 61% fiber launching efficiency. As shown in Fig. 2(e), the wide-range spectrum, measured from a wide-range spectrometer (WaveScan-Extended IR, APE), clearly shows the residual 1.55 μm input, the 1.2 μm DW and frequency-shifted solitons in the 1.7–2.0 μm longer wavelength regime. From the spectral measurement of Fig. 2(e), the wavelength range of DW was from 1000$\sim$1300 nm. And in this experiment, the DW conversion efficiency, defined as the power ratio between the $1.0 \sim 1.3$ μm DW band and the $1.0 \sim 2.5$ μm entire band, was 54.18%. With a 103 mW total average power at fiber output, the average power of femtosecond DW radiation was 55.9 mW, which corresponding to a 1.07 nJ pulse energy. Fig. 2(f) shows the 1.2 μm DW was with a 125 fs pulse width, corresponding to an 8.56 kW peak power. The polarization state of the 1.2 μm DW depends on the total birefringence of the fiber when the experiences were performed and it can be tuned to linearly polarized by a fiber-based polarization controller and a polarization beam splitter cube.

For generating DW radiations in other wavelength regime, the optimized parameters between source and the given NLF, the performances can be numerically simulated by solving the non-linear Schrodinger equations [27] before performing experiments. With a given NLF and a fixed femtosecond laser, the rule of thumb to raise the pulse energy of DW radiations was utilizing an ultrashort femtosecond pulses as discussed by [17].

4. Application of the Fiber-Based Femtosecond Source on Nonlinear Light Microscopy

A fiber-delivered two-photon-fluorescence (TPF) and second-harmonic-generation (SHG) microscope was set up based on the demonstrated fiber-based 1.2 μm femtosecond DW sources. From the previous report [28], TPF occurs in fluorescent molecules, such as the chloroplast within the mesophyll cells within the leaf [12], [29], and SHG occurs in optically non-center-symmetric media, such as collagen fibrils [7], [30].

In the experiment, the NLF output (point C in Fig. 1) was directly connected to the input end of an Olympus FV300 scanning system combined with an Olympus BX53 upright microscope where all optics were modified to allow the passage of the 1.2 μm femtosecond pulses. The microscopy system has a 40% transmission coefficients to the 1.2 μm radiation. On the other hand, the microscope and the focusing objective are with high-losses to the residual 1.55 μm radiations generated by the laser. The fundamental frame rate of the FV-300 NLM system was 1 frame per second. And the image pixel size in this experiment was 256 by 256. The utilized biological samples for demonstrating TPF and SHG microscopes were the leaf of Macrothelypteris Torresiana and type I collagen, respectively. A water immersion objective (UPlanSApo 60XW, Olympus, Japan) with a 1.2 NA was utilized to focus the laser beam into the sample. The generated TPF and SHG signals were back-scattered and detected by a photo-multiplication tube. A band-pass filter was placed before the PMT to pass the TPF signals from the mesophyll tissues in the TPF microscope. Another BPF was used to filter out the SHG signals from the collagens in the SHG microscope. Fig. 3(a) shows the TPF images of mesophyll tissues in the leaf of Macrothelypteris Torresiana and the chloroplast distributions inside the mesophyll cells can be identified with a sub-micron resolution. On the other hand, Fig. 3(b) shows the SHG images of type I collagen, where the distribution of collagen can be clearly resolved. The image sizes in the TPF and SHG microscope were both 100 μm by 100 μm. Both images were acquired within tens of micrometers below the surface of specimen.
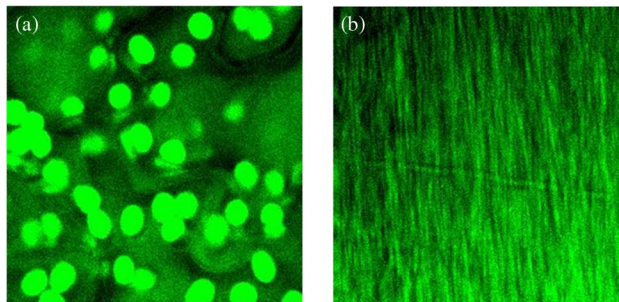
Fig. 3. (a) TPF images for the mesophyll tissues in the leaf of Macrothelypteris Torresiana. (b) SHG microscope images of type I collagen. The image size of both figures were 100 μm by 100 μm.

In the present demonstrated 1.2 μm fiber-based femtosecond source, up to a 54.9 mW output power (1.07 nJ pulse energy), mainly limited by the available pumping single-mode laser diode and EDFA, was reached. For some NLM applications, this power level is sufficient. For future *in vivo* or endoscopic NLM requiring high speed, multi-parallel excitation, or a higher penetration depth, the fiber-based laser sources working within the 1.2–1.3 μm bio-penetration window with a higher output power (up to several hundreds of milli-Watt) will be necessary. This issue can be addressed by a higher power 1.55 μm femtosecond fiber-laser source as excitation. Currently, high-power fiber-optical amplifier with a Watt-level output was developed by double-cladding-pumping technology so that the output power of 1.55 μm femtosecond fiber-laser could be scaled up and commercially available [4]. And with higher pulse energy, the parameters for evaluating the nonlinear interactions between energetic femtosecond pump pulses and nonlinear wavelength conversion fiber, including the dispersion length and nonlinear length, at specific condition should be carefully calculated or simulated to determine the optimum length of the nonlinear fiber [20].Third, the only free-space part, showing in the point B in Fig. 1, in this demonstrated source can be replaced by proper fiber slicing technology as shown in [18]. This demonstration shows the first step toward all-fiber-based femtosecond light source within the bio-penetration window for future NLM. The improved version of our source with a higher power was currently being developed and hopefully to be applied with clinical fiber-based endoscopes in the near future. Finally, in the present NLM system, the penetration depth was on the order of tens of μm below the surface of specimen. The penetration depth can be raised up by increasing the power of the DW source, by pulse compression, and by increasing the numerical aperture of the focusing objective in the NLM.

5. Conclusion

In conclusion, by merging three distinct research fields, including passively mode-locked fiber lasers, nonlinear fiber optics, and nonlinear light microscopy, we have demonstrated a compact and self-started fiber-based 1.2 μm femtosecond DW light source based on a high power 1.55 μm femtosecond fiber laser and a fiber-optic wavelength convertor. The 1.2 μm femtosecond light source, working within the bio-penetration window, delivered femtosecond pulses with a ~nJ level pulse energy, an average power in multi-tens of milliwatt-level and a pulse-duration of 125-fs. Then, with the simple, low-cost, and fiber-based 1.2 μm femtosecond source, intrinsic two-photon fluorescence microscopy and second-harmonic generation microscopy of leaf of Macrothelypteris Torresiana and type I collagen were performed for demonstration example. From the experimental results, the combination of passive mode-locked fiber-lasers and nonlinear fiber-optic wavelength convertors show great promise for future possible applications in NLM.

References

[1] W. Denk, J. H. Strickler, and W. W. Webb, "2-photon laser scanning fluorescence microscopy," *Science*, vol. 248, no. 4951, pp. 73–76, Apr. 1990.

[2] J. M. Squirrell, D. L. Wokosin, J. G. White, and B. D. Bavister, "Long-term two-photon fluorescence imaging of mammalian embryos without compromising viability," *Nature Biotechnol.*, vol. 17, no. 8, pp. 763–767, Aug. 1999.

[3] D. Kobat *et al.*, "Deep tissue multiphoton microscopy using longer wavelength excitation," *Opt. Exp.*, vol. 17, pp. 13 354–13 364, Aug. 2009.

[4] N. G. Horton *et al.*, "In vivo three-photon microscopy of subcortical structures within an intact mouse brain," *Nat. Photon.*, vol. 7, no. 3, pp. 205–209, Mar. 2013.

[5] S.-H. Chia *et al.*, "Miniaturized video-rate epi-third-harmonic-generation fiber-microscope," *Opt. Exp.*, vol. 18, no. 16, pp. 17 382–17 391, Aug. 2010.

[6] C.-K. Sun *et al.*, "Higher harmonic generation microscopy for developmental biology," *J. Struct. Biol.*, vol. 147, no. 1, pp. 19–30, Jul. 2004.

[7] R. M. Williams, W. R. Zipfel, and W. W. Webb, "Interpreting second-harmonic generation images of collagen I fibrils," *Biophys. J.*, vol. 88, no. 2, pp. 1377–1386, Feb. 2005.

[8] R. Tanaka *et al.*, "In vivo visualization of dermal collagen fiber in skin burn by collagen-sensitive second-harmonic-generation microscopy," *J. Biomed. Opt.*, vol. 18, no. 6, Jun. 2013, Art. ID. 061231.

[9] A. Zumbusch, G. R. Holtom, and X. S. Xie, "Three-dimensional vibrational imaging by coherent anti-Stokes Raman scattering," *Phys. Rev. Lett.*, vol. 82, no. 20, pp. 4142–4145, May 1999.

[10] C. W. Freudiger *et al.*, "Label-free biomedical imaging with high sensitivity by stimulated raman scattering microscopy," *Science*, vol. 322, no. 5909, pp. 1857–1861, Dec. 2008.

[11] R. R. Anderson and J. A. Parrish, "The optics of human skin," *J. Invest. Dermatol.*, vol. 77, no. 1, pp. 13–19, Jul. 1981.

[12] M.-C. Chan, T. M. Liu, S. P. Tai, and C. K. Sun, "Compact fiber-delivered Cr: Forsterite laser for nonlinear light microscopy," *J. Biomed. Opt.*, vol. 10, no. 5, Sep./Oct. 2005, Art. ID. 054006.

[13] D. J. Richardson, J. Nilsson, and W. A. Clarkson, "High power fiber lasers: Current status and future perspectives [Invited]," *J. Opt. Soc. Amer. B, Opt. Phys.*, vol. 27, no. 11, pp. B63–B92, Nov. 2010.

[14] H.-W. Chen *et al.*, "Chirally-coupled-core Yb-fiber laser delivering 80-fs pulses with diffraction-limited beam quality warranted by a high-dispersion-mirror based compressor," *Opt. Exp.*, vol. 18, no. 24, pp. 24 699–24 705, Nov. 2010.

[15] J. Xu, J. Liu, S. Wu, Q.-H. Yang, and P. Wang, "Graphene oxide mode-locked femtosecond erbium-doped fiber lasers," *Opt. Exp.*, vol. 20, no. 14, pp. 15 474–15 480, Jun. 2012.

[16] P. Wan, L.-M. Yang, and J. Liu, "High power 2 μm femtosecond fiber laser," *Opt. Exp.*, vol. 21, no. 18, pp. 21 374–21 379, Sep. 2013.

[17] G. Q. Chang, L. J. Chen, and F. X. Kartner, "Highly efficient Cherenkov radiation in photonic crystal fibers for broadband visible wavelength generation," *Opt. Lett.*, vol. 35, no. 14, pp. 2361–2363, Jul. 2010.

[18] X. M. Liu *et al.*, "All-fiber femtosecond Cherenkov radiation source," *Opt. Lett.*, vol. 37, no. 13, pp. 2769–2771, Jul. 2012.

[19] J. Takayanagi, T. Sugiura, M. Yoshida, and N. Nishizawa, "1.0–1.7-μm wavelength-tunable ultrashort-pulse generation using femtosecond Yb-doped fiber laser and photonic crystal fiber," *IEEE Photon. Technol. Lett.*, vol. 18, no. 21, pp. 2284–2286, Nov. 2006.

[20] T. Cheng *et al.*, "Highly efficient tunable dispersive wave in a Tellurite microstructured optical fiber," *IEEE Photon. J.*, vol. 7, no. 1, Feb. 2015, Art. ID. 2200107.

[21] K. Tamura, H. A. Haus, and E. P. Ippen, "Self-starting additive pulse mode-locked Erbium fiber ring laser," *Electron. Lett.*, vol. 28, no. 24, pp. 2226–2228, Nov. 1992.

[22] H. A. Haus, K. Tamura, L. E. Nelson, and E. P. Ippen, "Stretched-pulse additive-pulse mode-locking in fiber ring lasers—Theory and experiment", *IEEE J. Sel. Quantum. Electron.*, vol. 31, no. 3, pp. 591–598, Mar. 1995.

[23] J. C. Diels and W. Rudolph, *Ultrashort Laser Pulse Phenomena*. San Diego, CA, USA: Academic, 1996.

[24] H. W. Chen *et al.*, "Optimization of femtosecond Yb-doped fiber amplifiers for high-quality pulse compression," *Opt. Exp.*, vol. 20, no. 27, pp. 28 672–28 682, Dec. 2012.

[25] [Online]. Available: http://fiber-optic-catalog.ofsoptics.com/item/optical–fibers/highly-nonlinear-fiber-optical-fibers1/hnlf-standard-highly-non-linear-fiber-modules

[26] J. W. Nicholson *et al.*, "All-fiber, octave-spanning supercontinuum," *Opt. Lett.*, vol. 28, no. 8, pp. 643–645, Apr. 2003.

[27] G. P. Agrawal, *Nonlinear Fiber Optics*. San Diego, CA, USA: Academic, 2007.

[28] S.-W. Chu *et al.*, "Multimodal nonlinear spectral microscopy based on a femtosecond Cr:forsterite laser," *Opt. Lett.*, vol. 26, no. 23, pp. 1909–1911, Dec. 2001.

[29] S. P. Tai *et al.*, "Two-photon fluorescence microscope with a hollow-core photonic crystal fiber," *Opt. Exp.*, vol. 12, no. 25, pp. 6122–6128, Dec. 2004.

[30] S. W. Chu *et al.*, "Thickness dependence of optical second harmonic generation in collagen fibrils," *Opt. Exp.*, vol. 15, no. 19, pp. 12 005–12 010, Sep. 2007.